N90-22654

<u>Program 2</u> **Elevated Temperature Crack Growth in Aluminum Alloys: Tensile Deformation of 2618 and FVS0812 Aluminum Alloys**

Yang Leng and Richard P. Gangloff

Objectives

The objectives of this portion of the project are:

1) to characterize the elastic-plastic deformation behavior of ingot metallurgy 2618 and powder metallurgy Al-Fe-V-Si alloys as function of temperature.

2) to investigate the correlation between tensile behavior and microstructure.

Program 2 — Elevated Temperature Crack Growth in Aluminum Alloys: Time Dependent Crack Growth Behavior of Alloy 2618

Yang Leng and Richard P. Gangloff

Objectives

The objectives of this program are to investigate the subcritical crack growth behavior of aluminum alloy 2618 at elevated temperatures, to determine the dominant damage mechanism and to correlate macroscopic crack growth with microstructure.

Time Dependent Crack Growth in Aluminum Alloys at Elevated Temperature

Yang Leng and Richard P. Gangloff
Department of Materials Science

Abstract

Understanding the damage tolerance of aluminum alloys at elevated temperatures is essential for safe applications of advanced materials. The objective of this project is to investigate the time dependent subcritical cracking behavior of powder metallurgy FVS0812 and ingot metallurgy 2618 aluminum alloys at elevated temperatures.

The fracture mechanics approach was applied in this study. Sidegrooved compact tension specimens were tested at 175, 250 and 316°C under constant load. Subcritical crack growth occurred in each alloy at applied stress intensity levels (K) of between about 14 and 25 MPa$\sqrt{m}$, well below K_{IC}. Measured load, crack opening displacement and displacement rate, and crack length and growth rate (da/dt) were analyzed with several continuum fracture parameters including, the C^*-integral, C_t and K. Since extensive creep conditions are not met according to the transition time criterion and for the load levels which produce crack growth, the C^*-integral is not a relevant parameter for these aluminum alloys. Elevated temperature growth rate data suggest that K is a controlling parameter during time dependent cracking. For FVS0812, da/dt is highest at 175°C when rates are expressed as a function of K. While crack growth rate is not controlled by C_t at 175°C, da/dt appears to better correlate with C_t at higher temperatures. Here, "creep brittle" cracking at intermediate temperatures, and perhaps related to strain aging, is augmented by time dependent transient creep plasticity at higher temperatures. The C_t analysis is, however, complicated by the necessity to measure small differences in the elastic crack growth and creep contributions to the crack opening displacement rate.

A microstructural study indicates that 2618 and FVS0812 are likely to be creep brittle materials, consistent with the results obtained from the fracture mechanics study. Time dependent crack growth of 2618 at 175°C is characterized by mixed transgranular and intergranular fracture. Delamination along the ribbon powder particle boundaries occurs in FVS0812 at all temperatures. The fracture mode of FVS0812 changes with temperature. At 175°C, it is characterized as dimpled rupture, and at 316°C as mixed matrix superplastic rupture and matrix-dispersoid debonding.

Further study will concentrate on revealing the correlation between macromechanical behavior and microstructure, investigating possible environmental effects and exploring mechanisms of time dependent crack growth in these advanced aluminum alloys.

Damage Tolerance of Advanced Aluminum Alloys

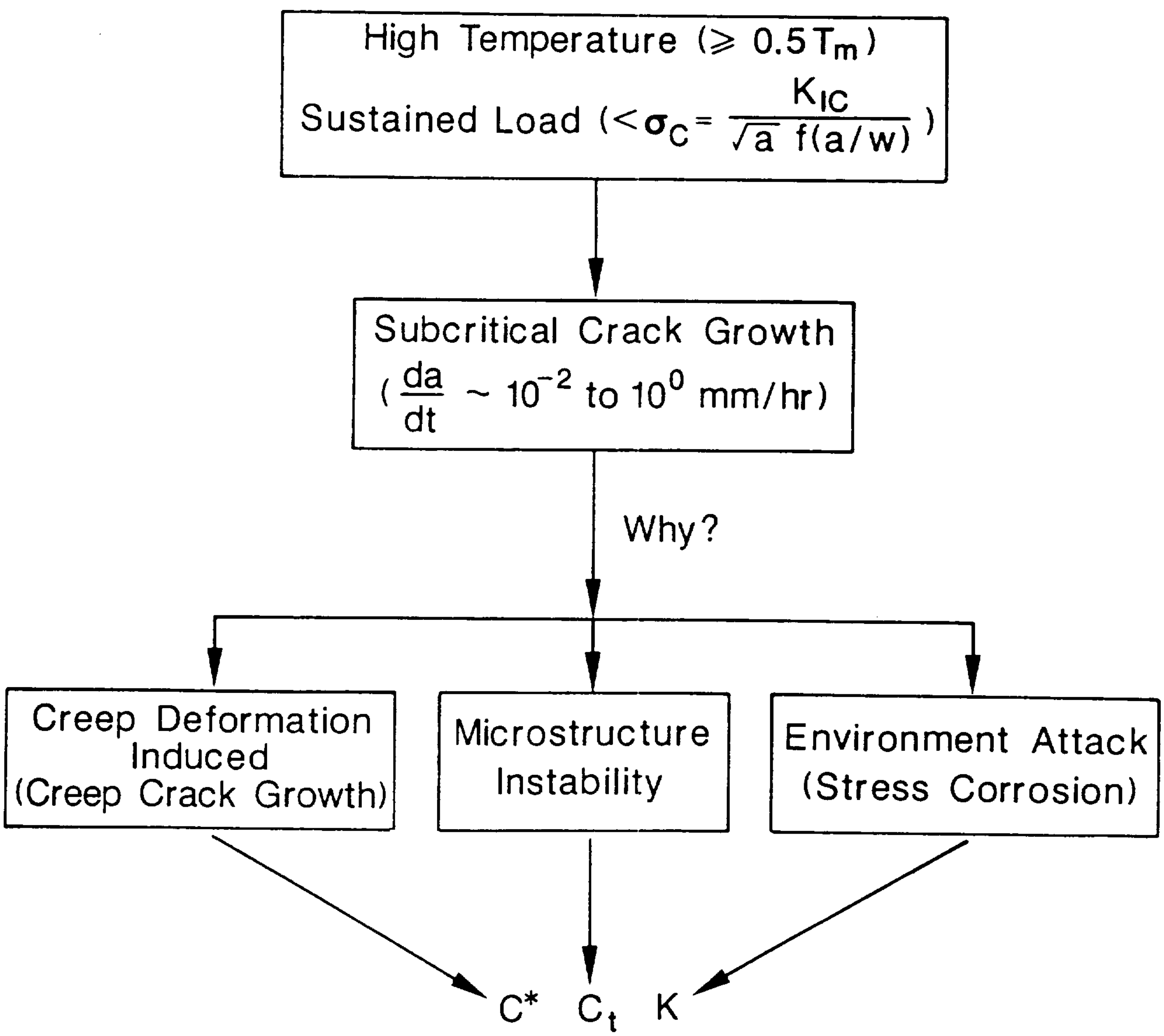

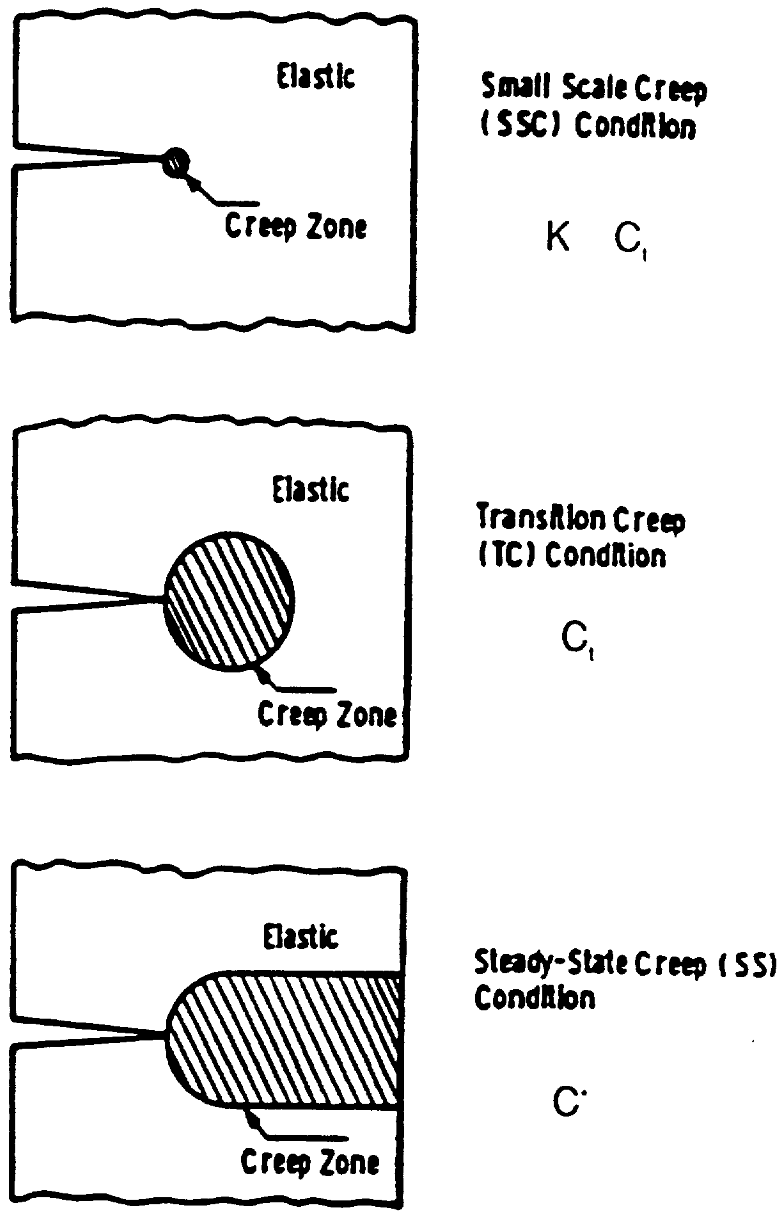

Elastic
Creep Zone
Small Scale Creep
(SSC) Condition
K C_t
Elastic
Creep Zone
Transition Creep
(TC) Condition
C_t
Elastic
Creep Zone
Steady-State Creep (SS)
Condition
C*

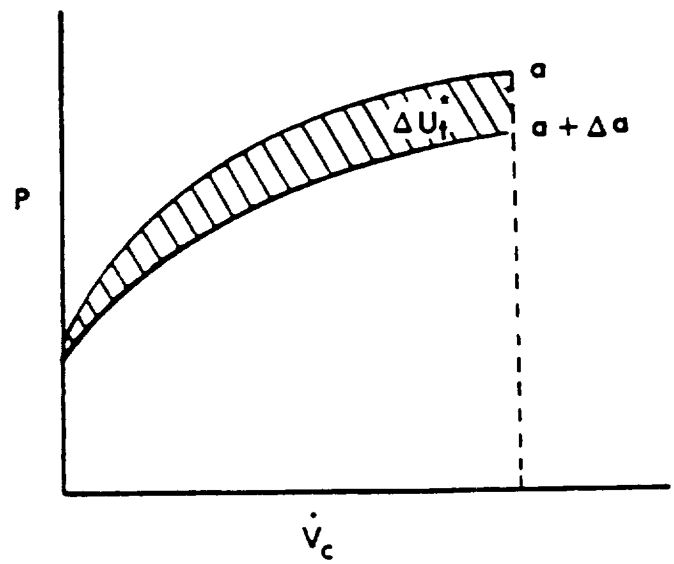

The C_t is an instantaneous energy rate dissipation rate which can characterize CCG from small scale to steady state creep

$$C_t = -\frac{1}{B}\frac{\partial \dot{U}_t}{\partial a}$$

For compact tension specimens

$$(C_t)_{ssc} = \frac{P\,\dot{V}_c}{B\,W}\frac{F'}{F}$$

F' and F are geometric factors and

$$\frac{F'}{F} = f(a/w)$$

TRANSITION TIME CRITERIA

$$t_T = \frac{K^2(1-\nu^2)}{E(n+1)C^*}$$

$$C^* = A_1 \frac{\sigma_o^2}{E}(W-a)\,h_1\left(\frac{P}{P_o}\right)^{n+1}$$

$$\dot{\varepsilon} = A_1\left(\frac{\sigma}{\sigma_o}\right)^n$$

The transition time can be used to justify the validity of C^*.
There is no analytical criteria to justify C_t and K.

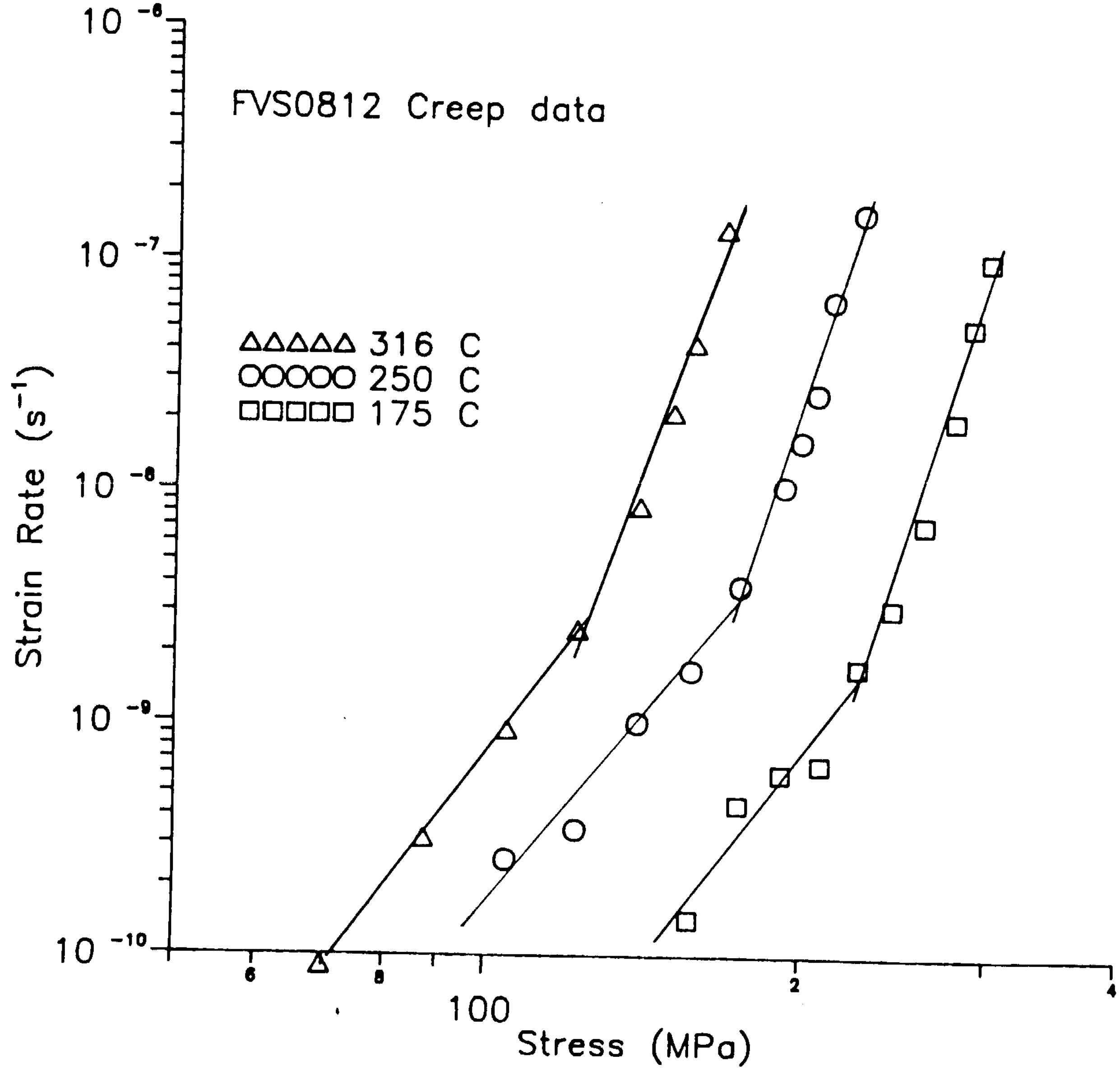

FVS0812 Creep data
316 C
250 C
175 C
Strain Rate (s^-1)
10^-6
10^-7
10^-8
10^-9
10^-10
6
8
100
2
4
Stress (MPa)

TRANSITION TIME FOR ALLOY ALLOYS

Material	temperature(°C)	n	t_T (year) a/W=0.5	t_T (year) a//W=0.6
2618	175	6.1	$1.7x10^2$	2.4
0812	175	5.9	$1.3x10^2$	19
0812	175	15	$1.2x10^6$	$3.2x10^3$
0812	250	5.4	12	2.2
0812	250	14	$7.8x10^3$	28
0812	316	5.9	3.9	.59
0812	316	12	84	.64

Applied load = 2.2 kN

The ratio of applied stress on ligament to yield strength is only about 4% to 8 %.

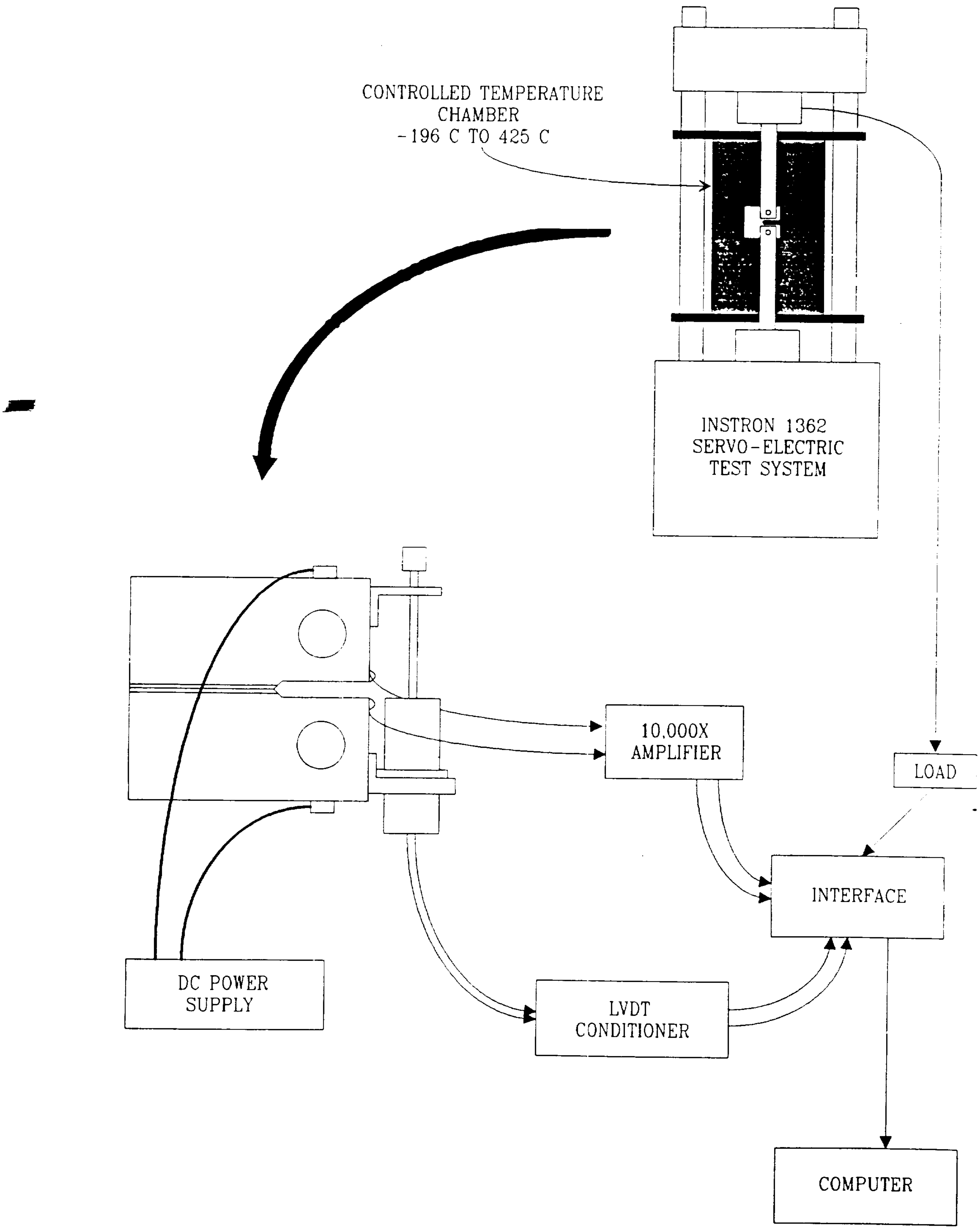
CONTROLLED TEMPERATURE
CHAMBER
-196 C TO 425 C
INSTRON 1362
SERVO-ELECTRIC
TEST SYSTEM
10,000X
AMPLIFIER
LOAD
INTERFACE
DC POWER
SUPPLY
LVDT
CONDITIONER
COMPUTER

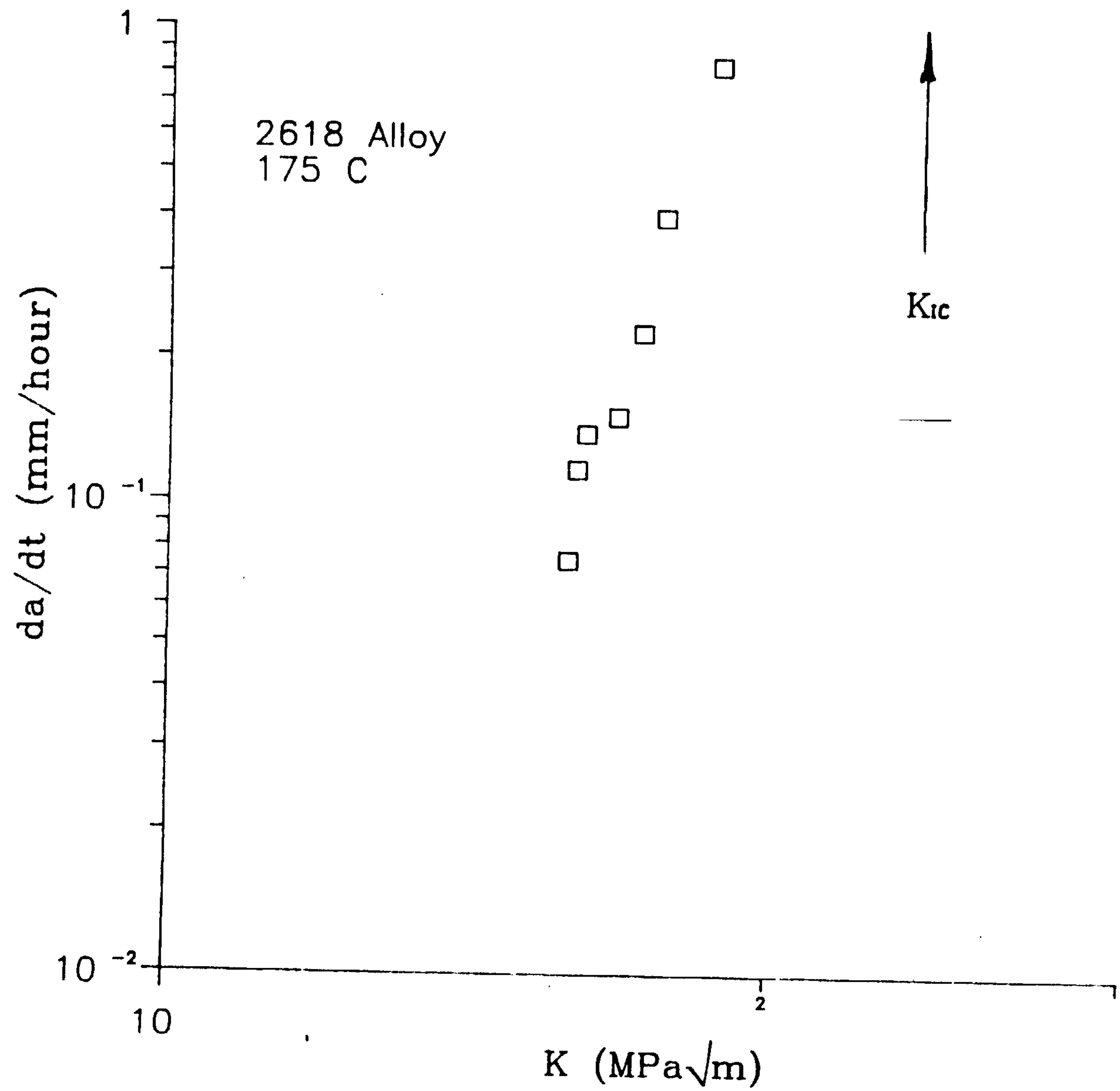

2618 Alloy
175 C
Kic
1
10 ⁻¹
10 ⁻²
10
2
da/dt (mm/hour)
K (MPa√m)

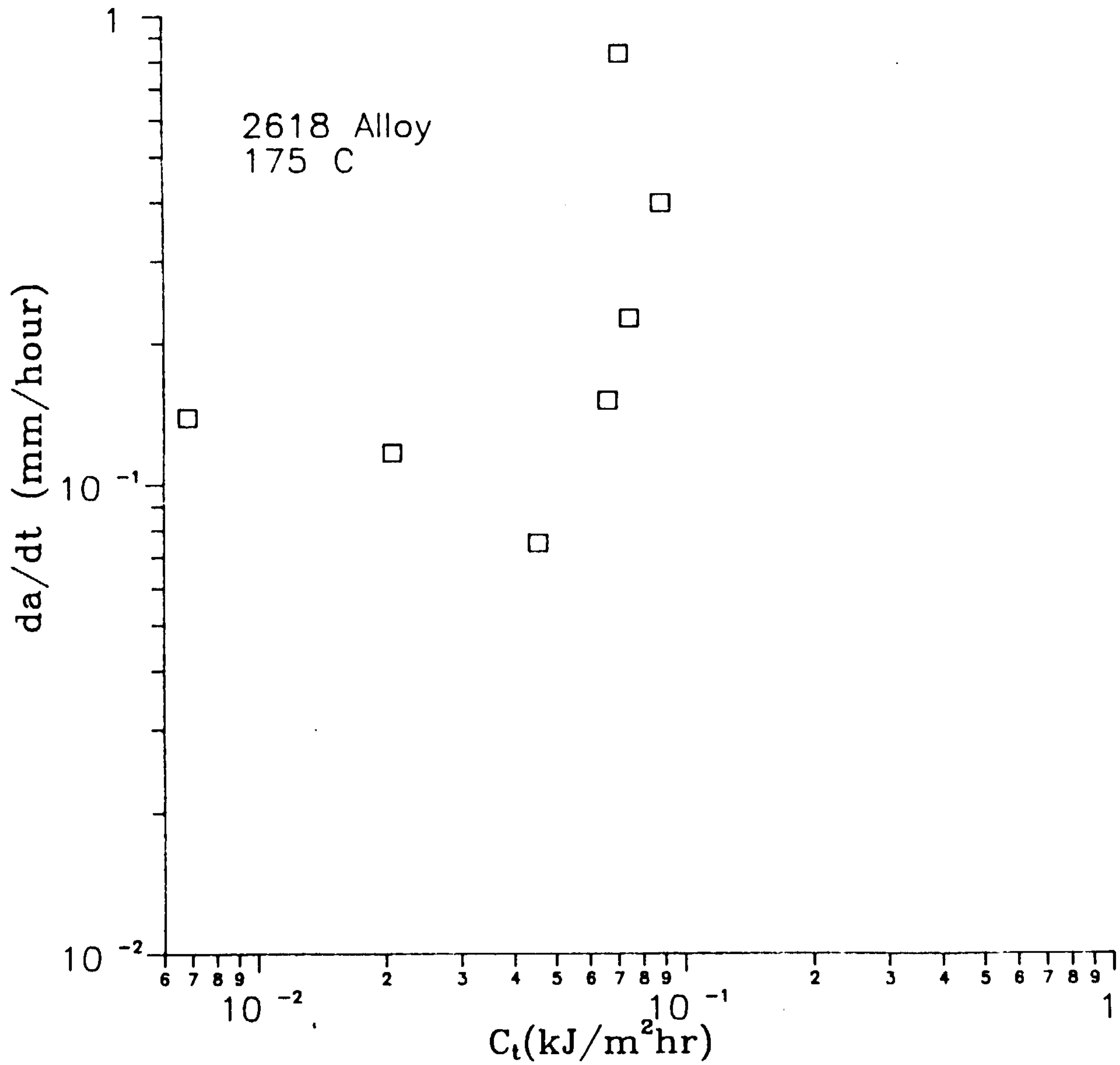

2618 Alloy
175 C
da/dt (mm/hour)
1
10^{-1}
10^{-2}
10^{-2}
10^{-1}
1
$C_t(kJ/m^2hr)$

For compact tension specimens

$$(C_t)_{ssc} = \frac{P\,\dot{V}_c}{B\,W}\frac{F'}{F}$$

Load line deflection rate, $\dot{V}$, can be partitioned into two components

$$\dot{V} = \dot{V}_e + \dot{V}_c$$

$\dot{V}_e$ = deflection rate corresponding to change in elastic compliance with crack growth

$\dot{V}_c$ = deflection rate due to development of creep deformation

Under constant load condition

$$\dot{V}_c = \dot{V} - \frac{\dot{a}B}{P}\left[\frac{2K^2}{E}\right]$$

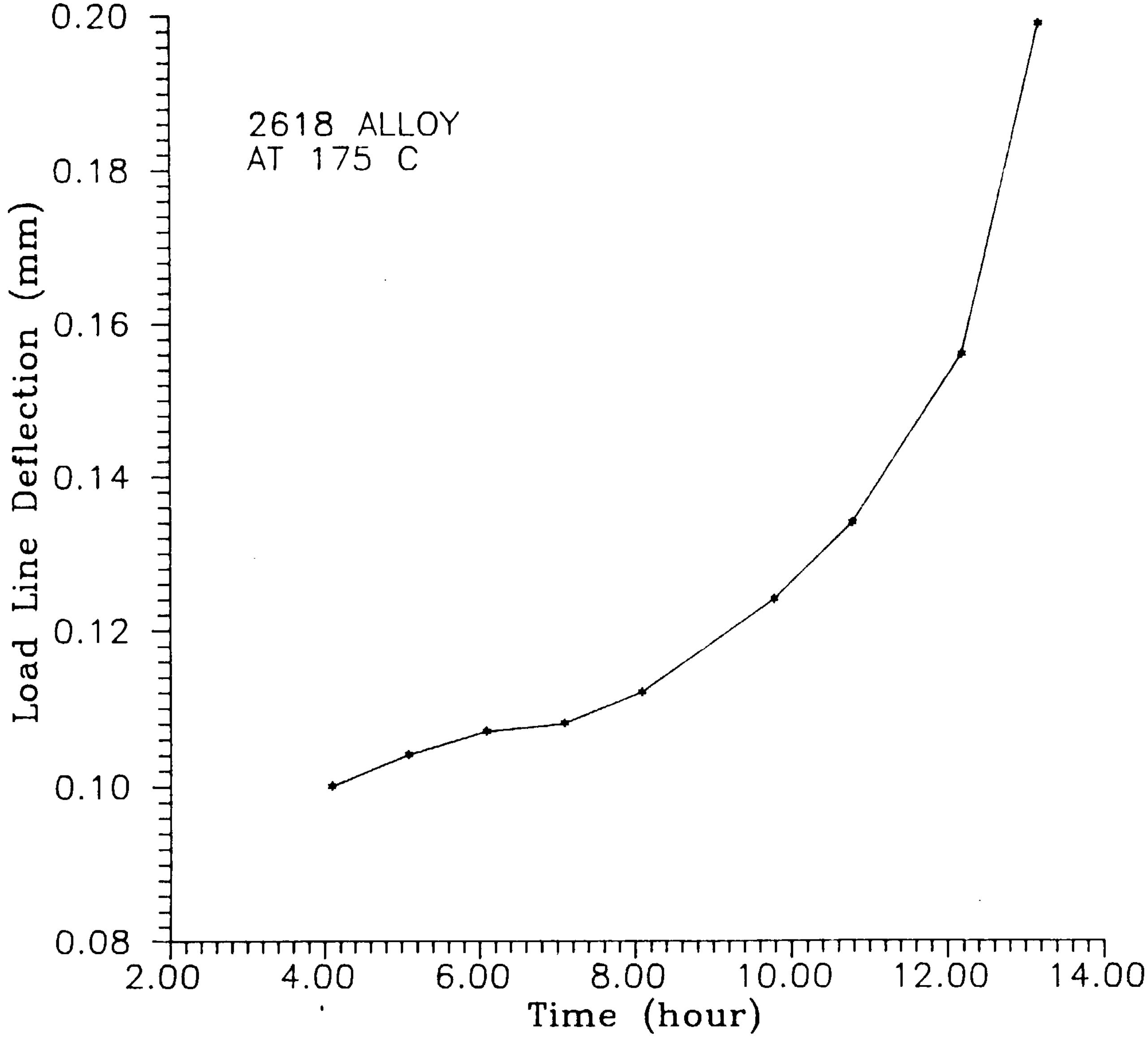

2618 ALLOY
AT 175 C
Load Line Deflection (mm)
0.20
0.18
0.16
0.14
0.12
0.10
0.08
2.00
4.00
6.00
8.00
10.00
12.00
14.00
Time (hour)

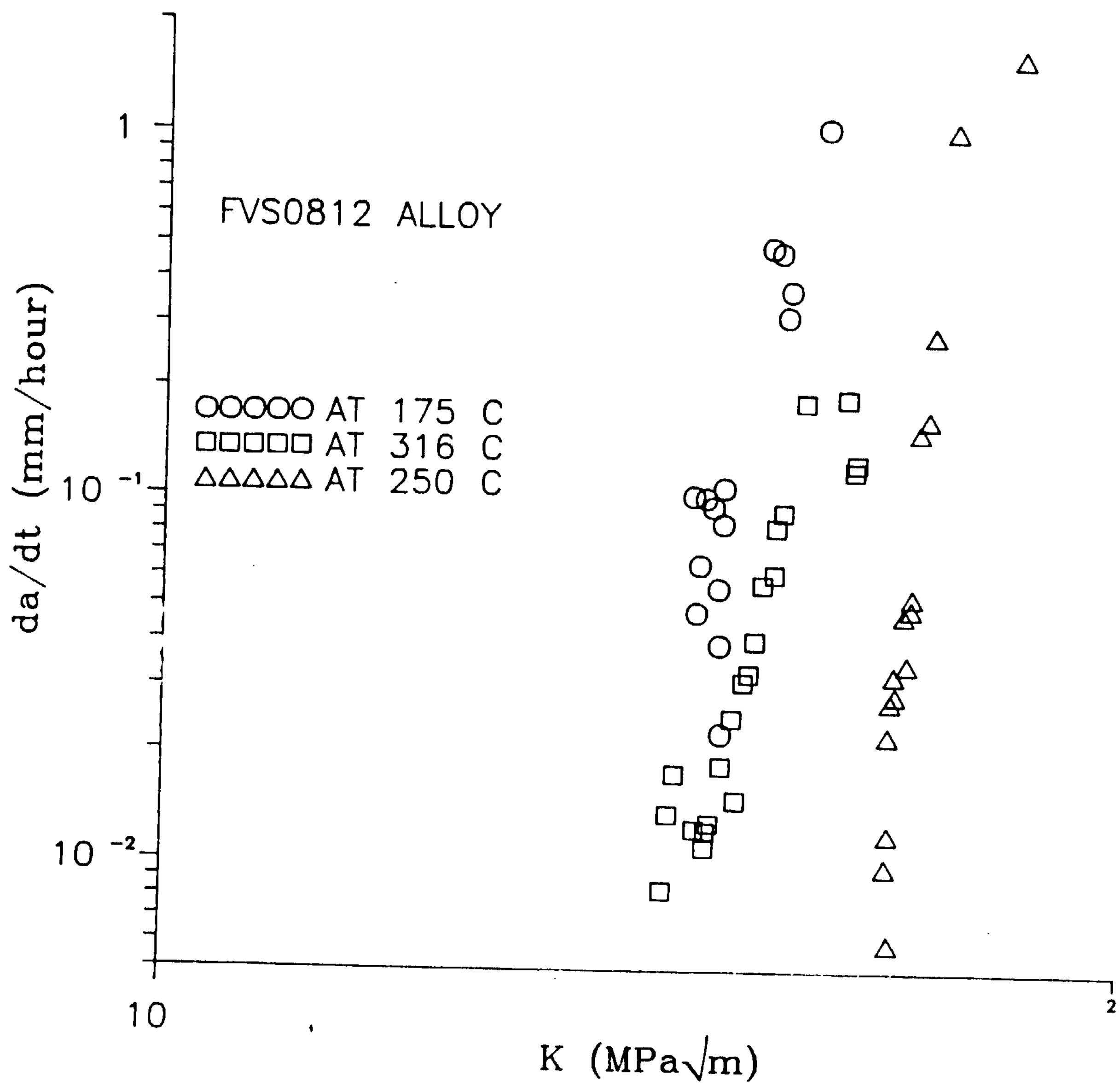

FVS0812 ALLOY
OOOOO AT 175 C
□□□□□ AT 316 C
ΔΔΔΔΔ AT 250 C
da/dt (mm/hour)
1
10 ⁻¹
10 ⁻²
10
2
K (MPa√m)

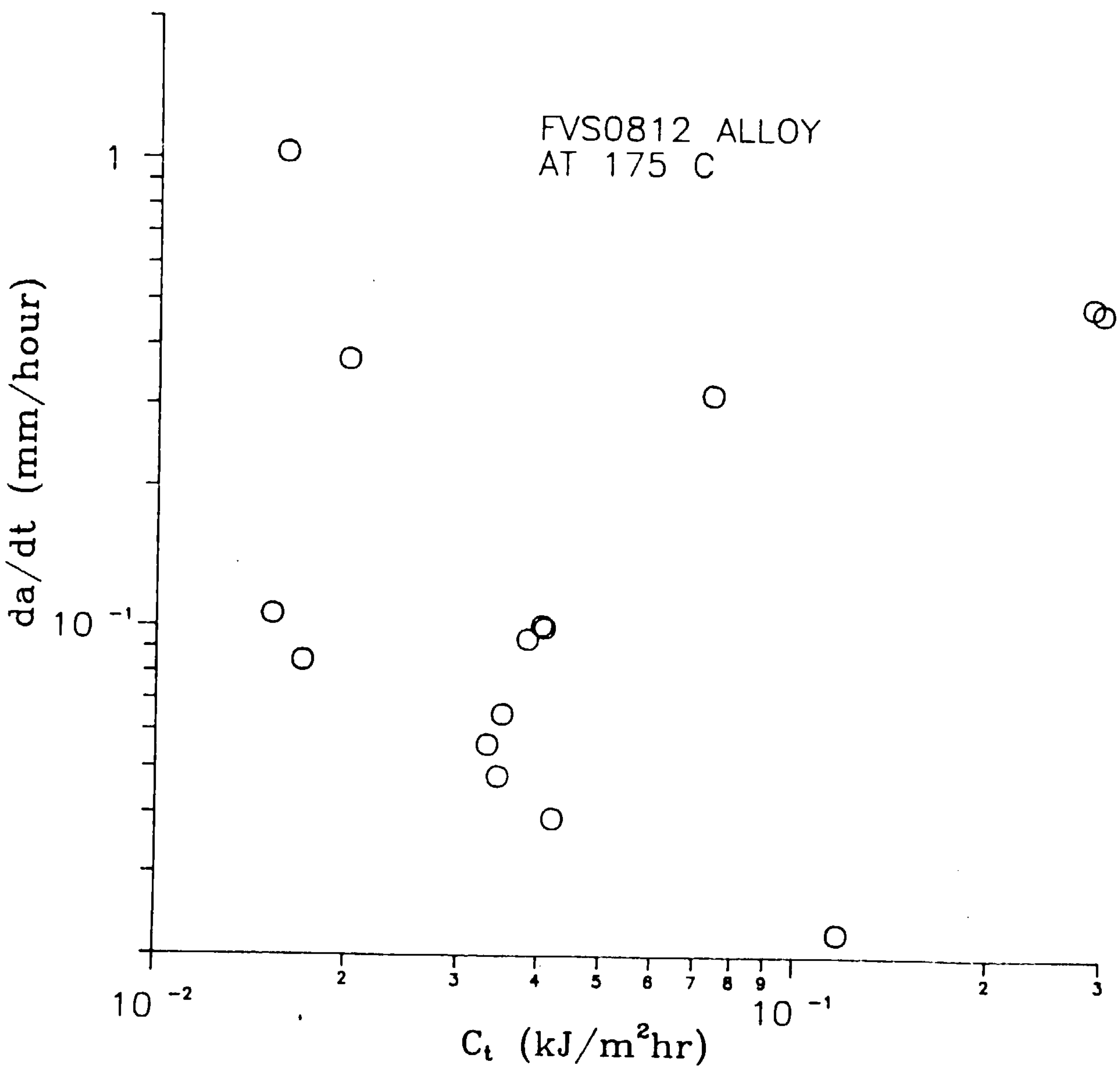

FVS0812 ALLOY
AT 175 C
da/dt (mm/hour)
1
10 ⁻¹
10 ⁻²
2
3
4
5
6
7
8
9
10 ⁻¹
2
3
C_t (kJ/m²hr)

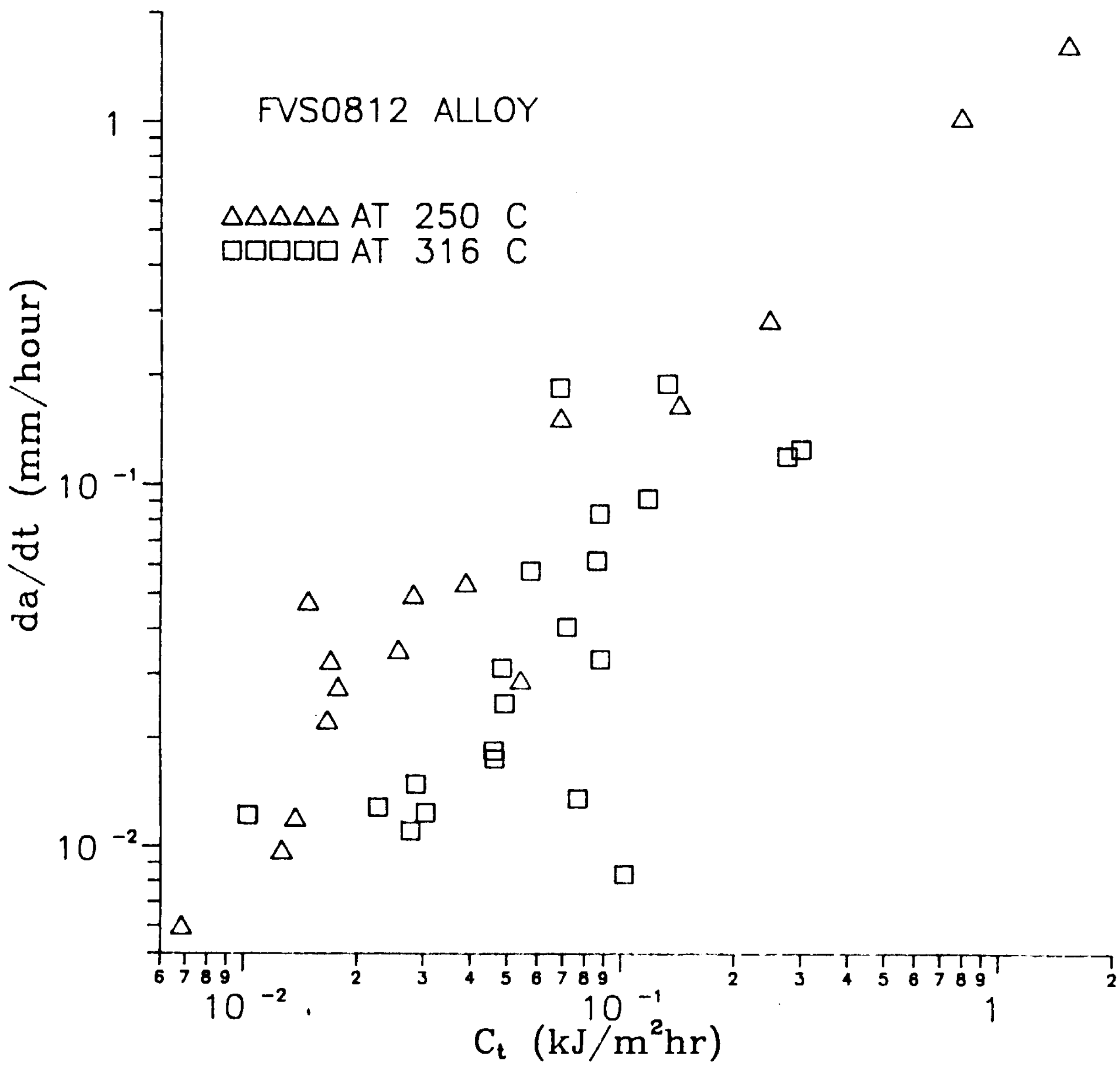

FVS0812 ALLOY
ΔΔΔΔΔ AT 250 C
□□□□□ AT 316 C
da/dt (mm/hour)
1
10 ⁻¹
10 ⁻²
6 7 8 9
2 3 4 5 6 7 8 9
2 3 4 5 6 7 8 9
2
10 ⁻²
10 ⁻¹
1
C_t (kJ/m²hr)

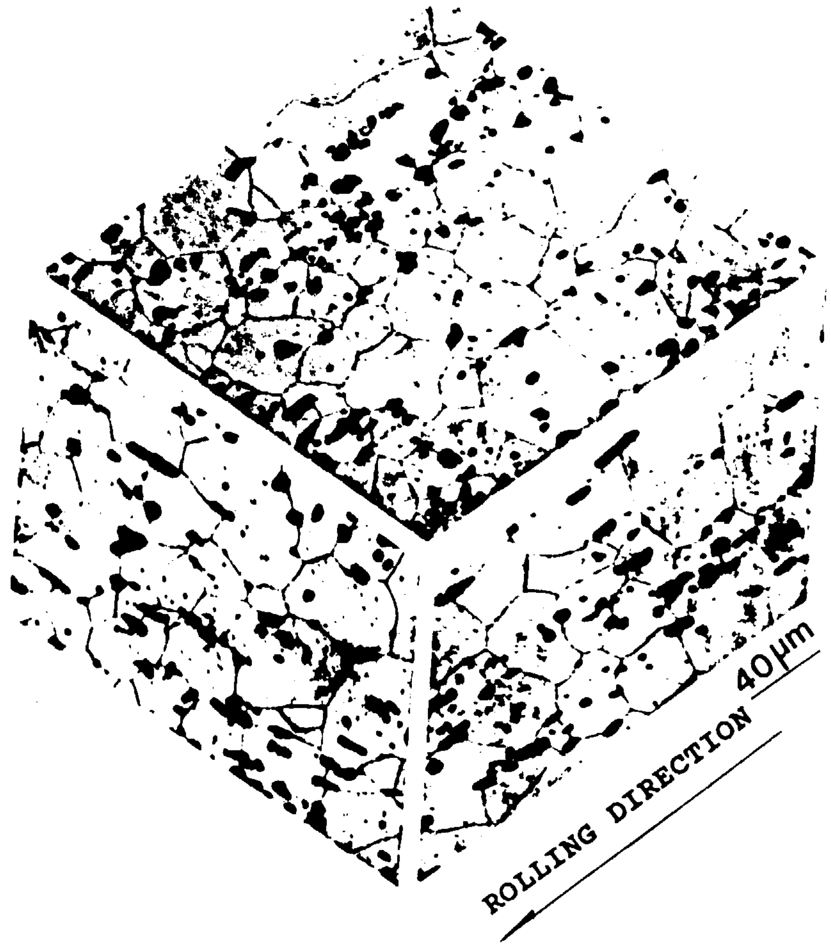

Optical micrograph of 2618 Al alloy

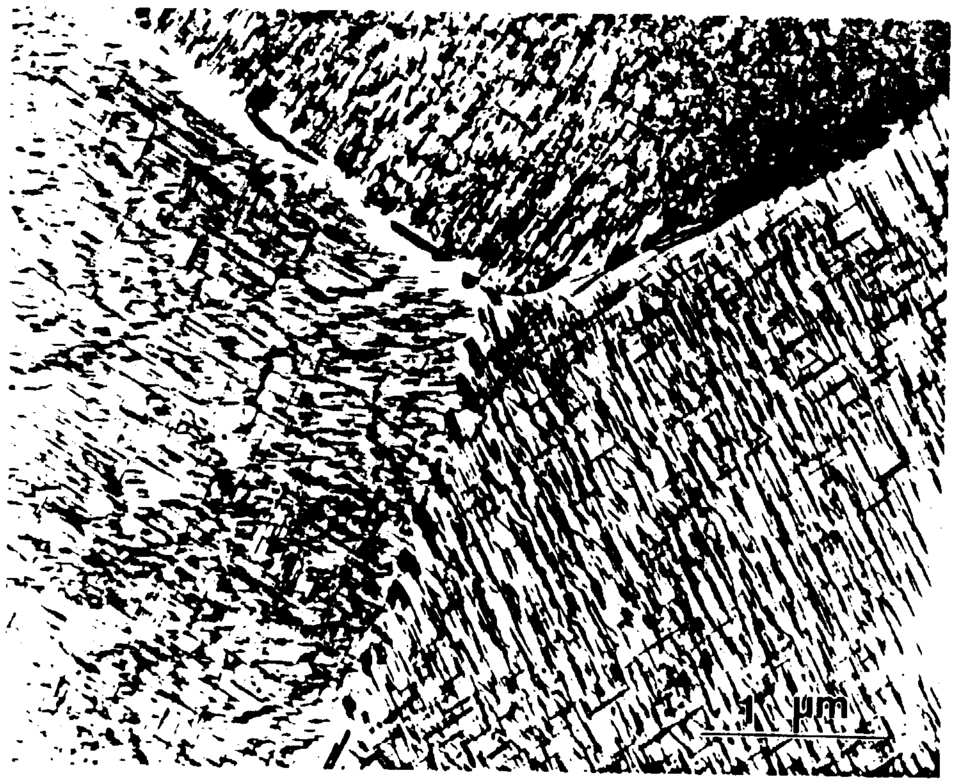

TEM micrograph of 2618 Al alloy

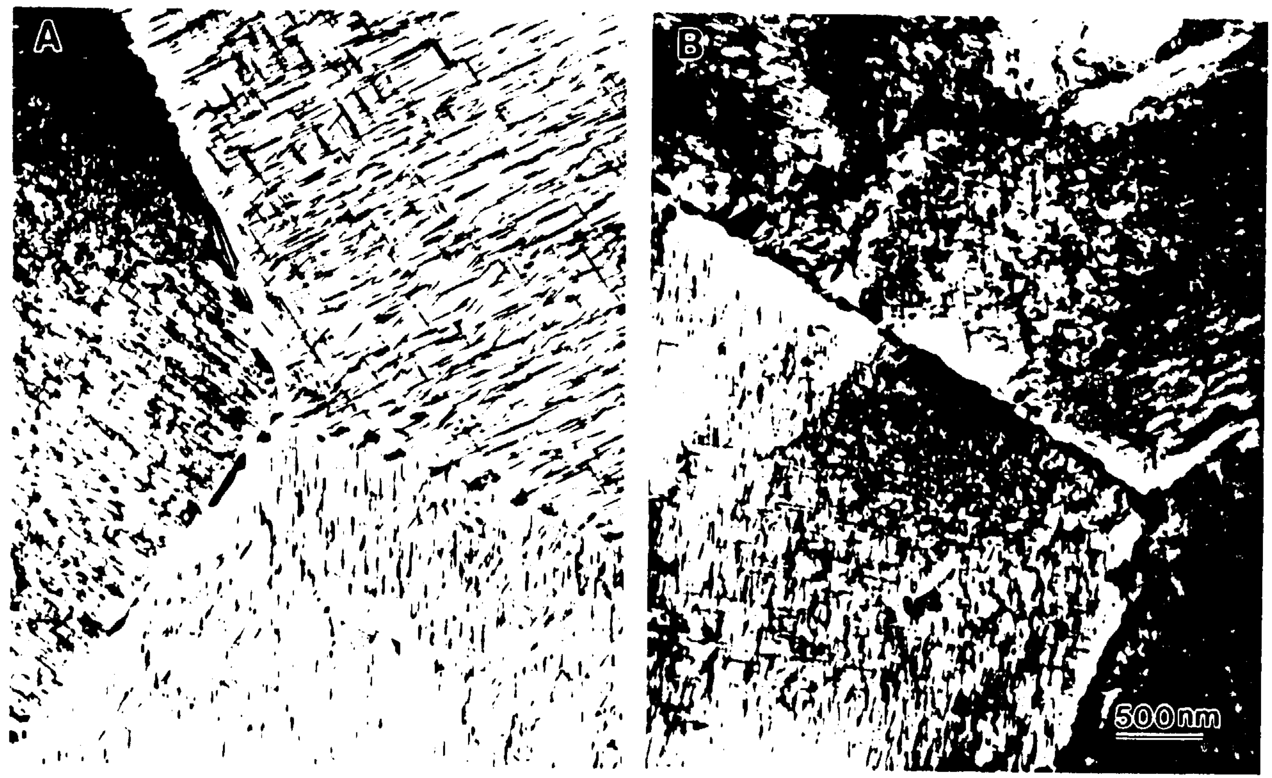

TEM micrographs of 2618 Al alloy a) room temperature
b) after heated to 300 °C for one hour

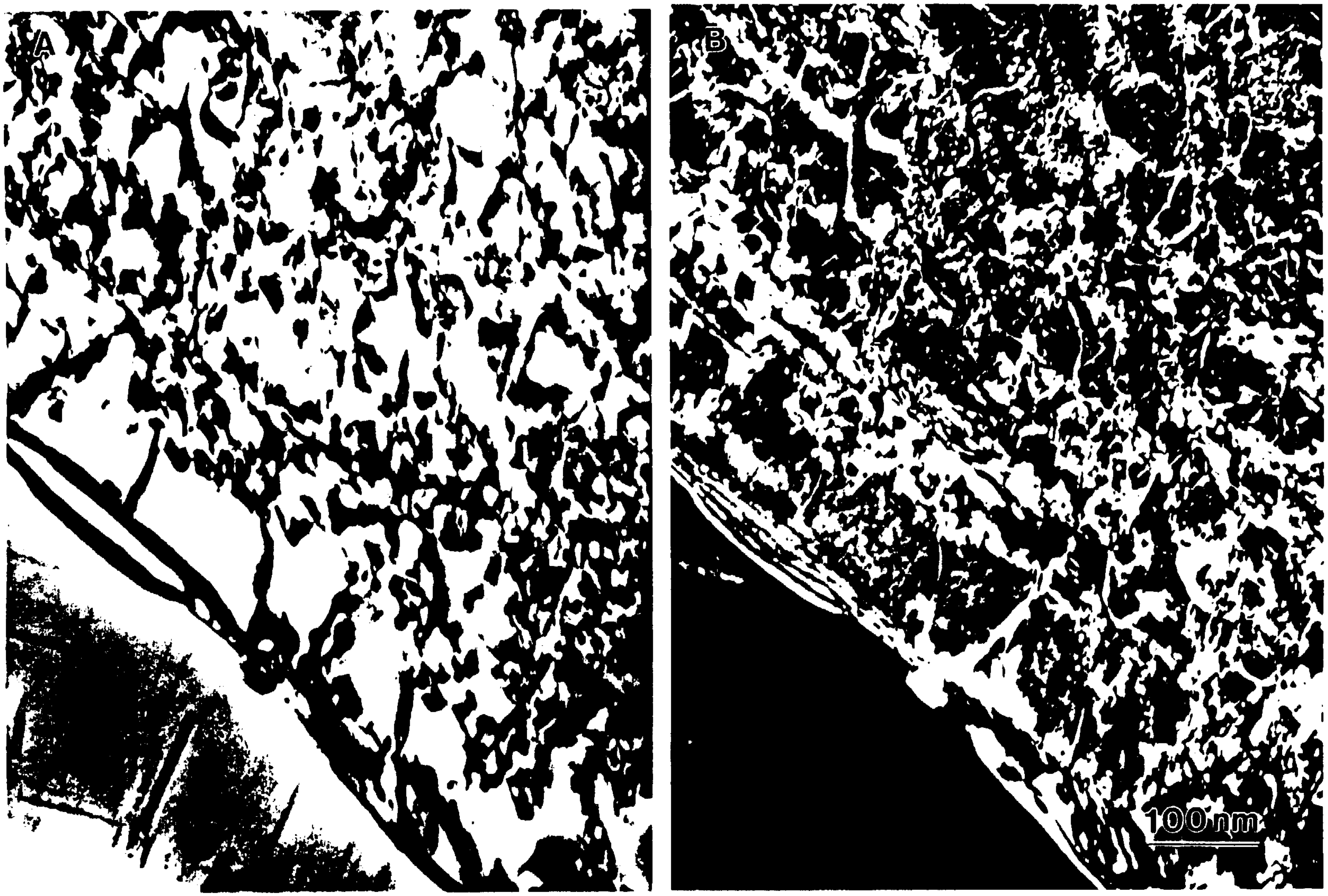

TEM micrographs of 2618 Al alloy after stretched to strain of 2%. The zone is [001]. a) bright field, b) weak beam dark field.

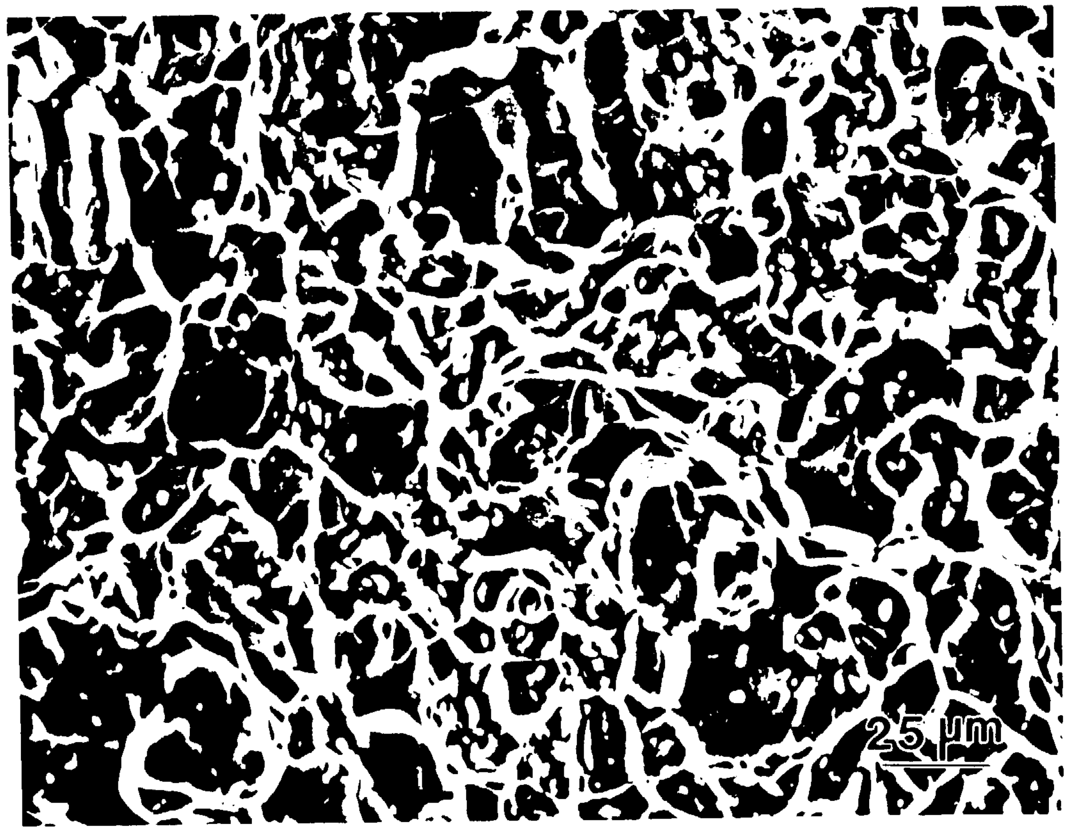

Creep crack growth fracture surface of 2618 Al alloy (175 °C)

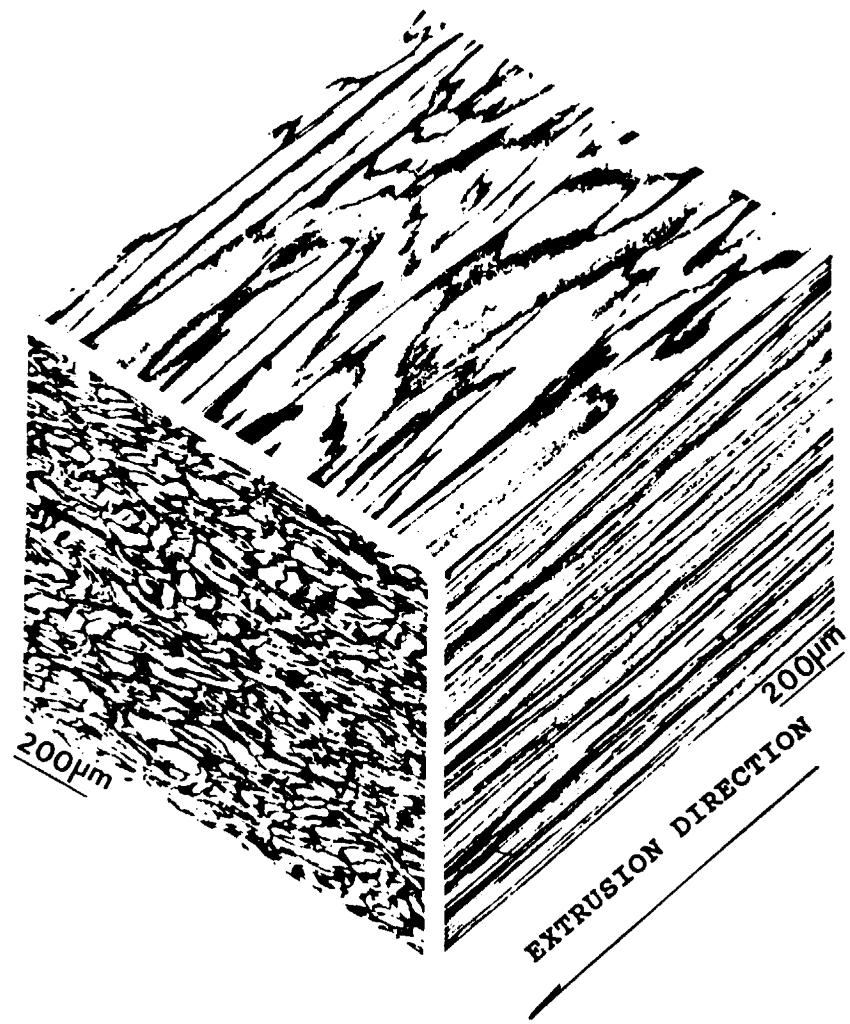

Optical micrographs (Bright field) of FVS0812 Al alloy

TEM micrograph of FVS0812 Al alloy

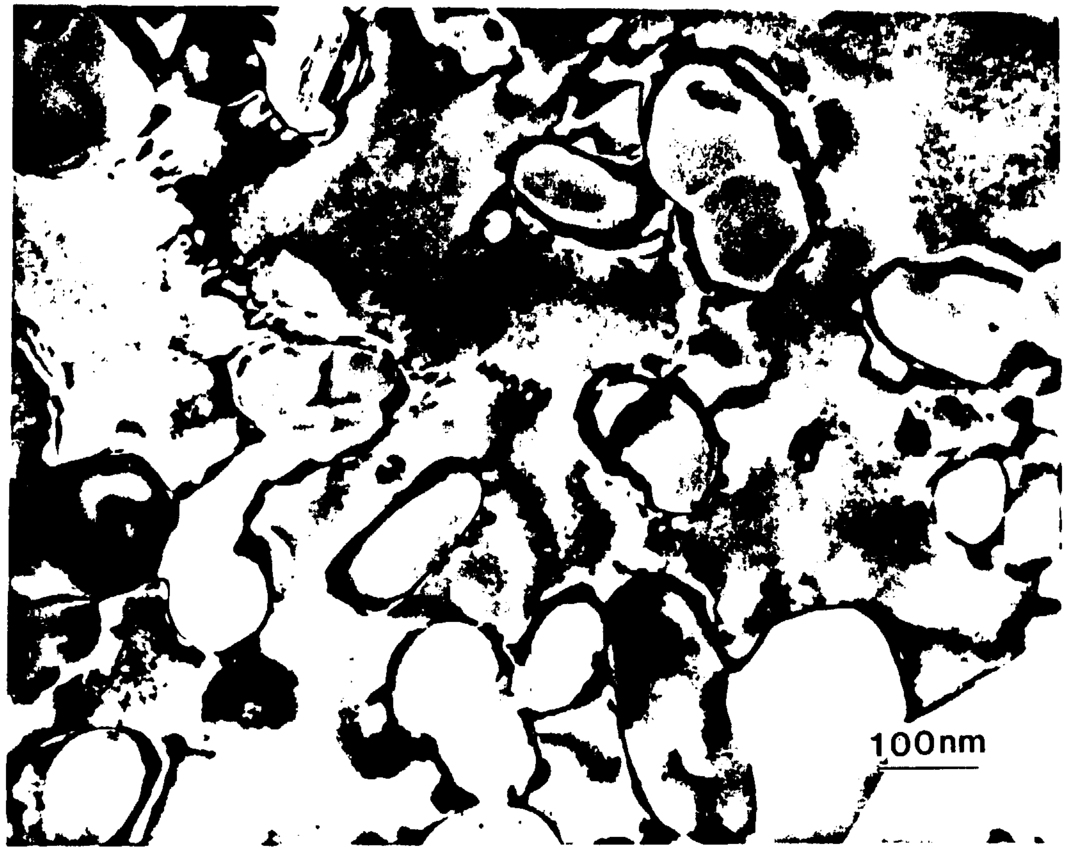

TEM micrograph of FVS0812 Al alloy after stretched to strain of 2%.

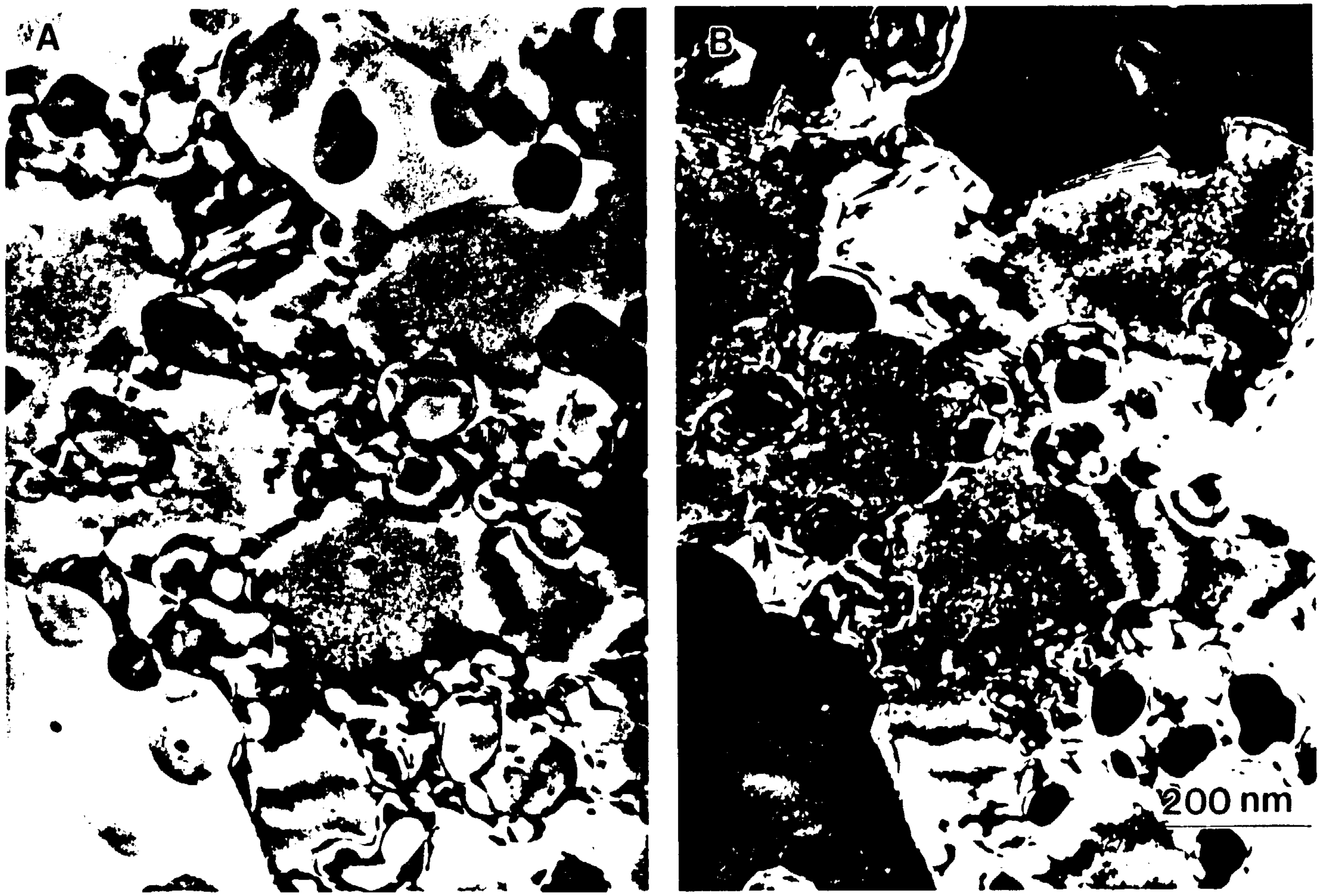

TEM micrographs of FVS0812 Al alloy after stretched to strain of 2%. a) bright field, b) weak beam dark field.

Creep crack growth fracture surface of FVS0812 (175 °C)

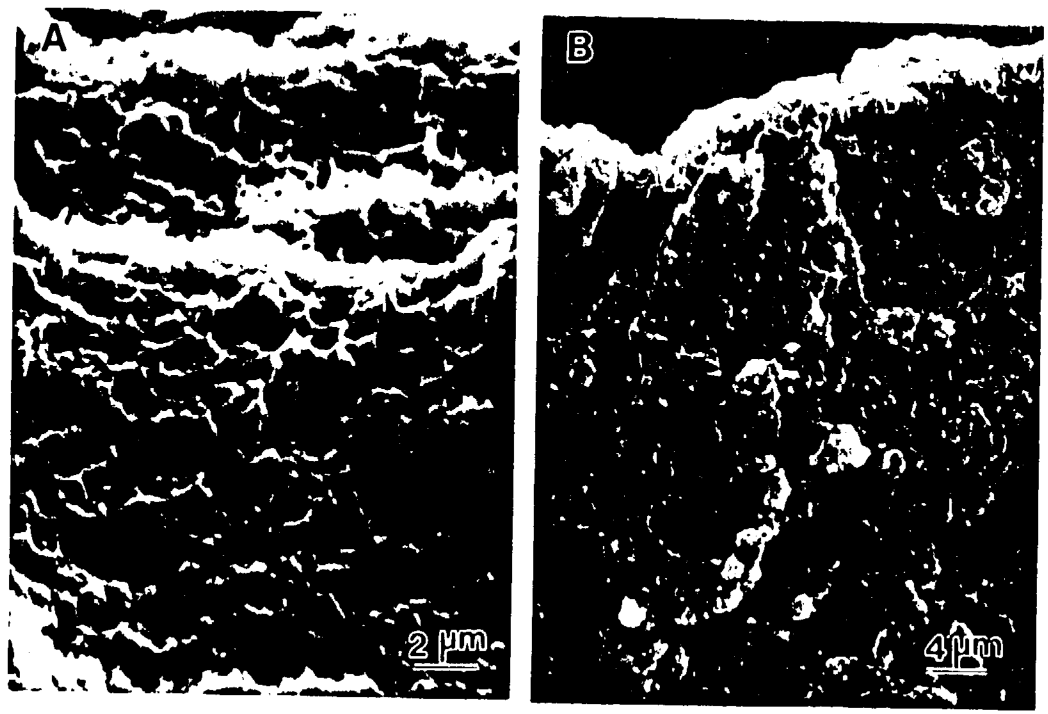

Side views of CCG fracture surface of FVS0812 (175 °C)
a) dimple fracture region   b) delamination region

Nomarski contrast micrograph of the crack path profile of FVS0812 Al alloy after creep crack growth tested at 316 °C

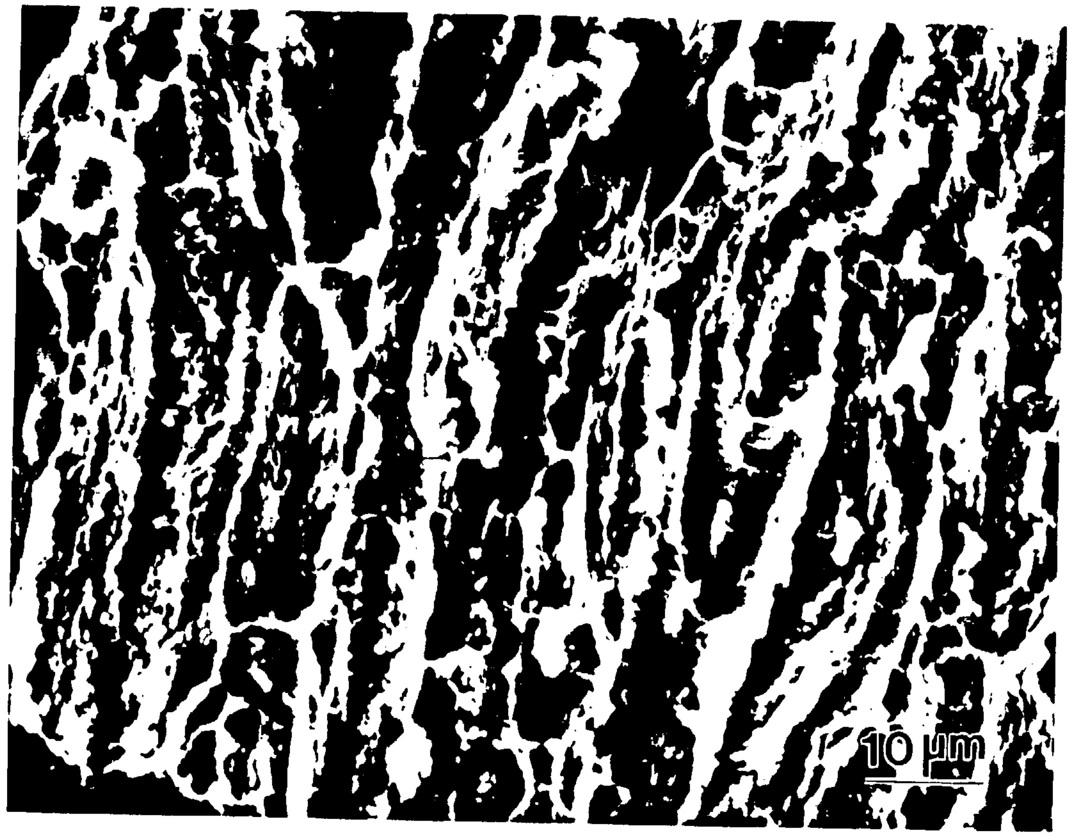

Creep crack growth fracture surface of FVS0812 (316 °C)

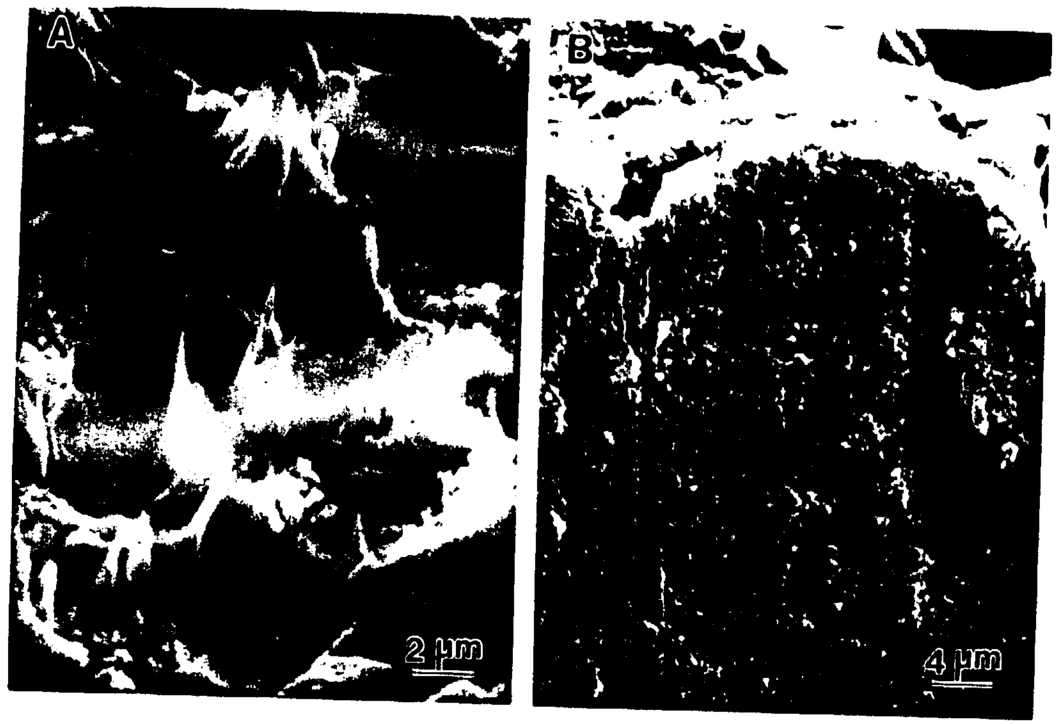

Side views of CCG fracture surface of FVS0812 (316 °C)
a) superplastic deformed and interdispersoid fracture region
b) delamination region

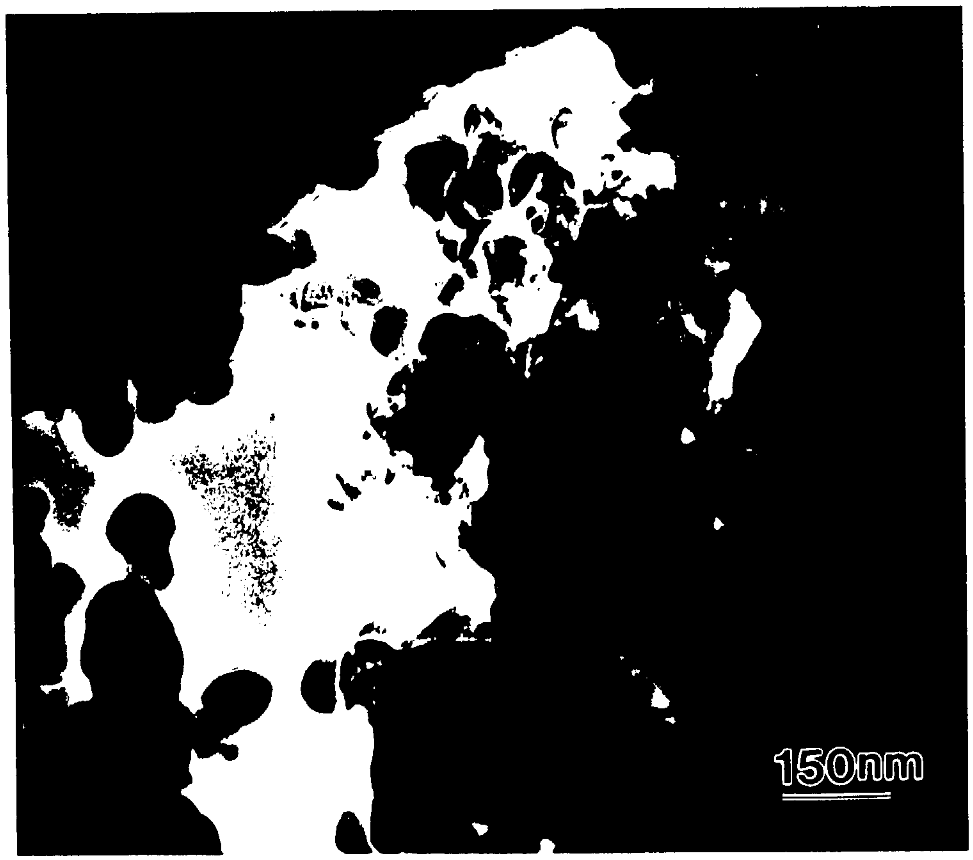

TEM micrograph of the crack tip of FVS0812 Al alloy after CCG tested at 316 °C

TEM micrograph of the crack tip of FVS0812 Al alloy after CCG tested at 316 °C